Identification of a Subpopulation of Binary Black Holes Formed Through Isolated Binary Evolution

Jaxen Godfrey,[1] Bruce Edelman,[1] and Ben Farr[1]

[1] *Institute for Fundamental Science, Department of Physics, University of Oregon, Eugene, OR 97403, USA*

ABSTRACT

Observations of gravitational waves (GWs) from merging compact binaries have become a regular occurrence. The continued advancement of the LIGO-Virgo-KAGRA (LVK) Collaboration detectors have now produced a catalog of over 90 such mergers, from which we can begin to uncover the formation history of merging compact binaries. In this work, we search for subpopulations in the LVK's third gravitational wave transient catalog (GWTC-3) by incorporating discrete latent variables in the hierarchical Bayesian inference framework to probabilistically assign each BBH observation into separate categories associated with distinctly different population distributions. By incorporating formation channel knowledge within the mass and spin correlations found in each category, we find an over density of mergers of with a primary mass of $\sim 10 M_\odot$, confidently associated with isolated binary formation. This low-mass subpopulation has a spin magnitude distribution peaking at $a_{\mathrm{peak}} = XX$, exhibiting spins preferentially aligned with the binary's orbital angular momentum, is constrained by $XX \pm XX$ of our observations, and contributes to $XX\%$ to the overall population of BBHs. While we cannot confidently identify the formation history of every event in the catalog, this work is a first step in gaining a deeper understanding of compact binary formation and evolution, and will provide more robust conclusions as the catalog of observations becomes larger.

1. INTRODUCTION

The first detection of gravitational waves (GWs) from a binary black hole (BBH) merger was made by the LIGO-Virgo-KAGRA (LVK) Collaboration on September 14, 2015. Since that fateful day, the LVK has detected nearly 100 compact binary coalescences (CBCs), bringing the third gravitational wave transient catalog (GWTC-3) up to 90 such events. (LIGO Scientific Collaboration et al. 2015; Acernese et al. 2015; Akutsu et al. 2021; Abbott et al. 2016, 2019a, 2021a; The LIGO Scientific Collaboration et al. 2021a). With the maturation of GW Astronomy, novel studies of the universe are possible; we are now able to probe the entire population of merging compact objects in the universe with much greater fidelity than with the sparse, early LVK catalogs (Abbott et al. 2019b, 2021b; The LIGO Scientific Collaboration et al. 2021b). By breaking down the full CBC population into subpopulations based on different source properties- and paired with our theoretical knowledge of stellar astrophysics- we can begin to uncover the formation and evolution of compact binaries (Zevin et al. 2017). The two most common expected

formation channels of merging compact objects are isolated formation and dynamical assembly, each predicted to produce binary populations with unique mass and spin characteristics (Farr et al. 2017, 2018; Arca Sedda et al. 2020). The uncertainty in modeled merger rates of each formation channel is large, and the predictions continue to evolve with better understanding of the underlying physics (see Mandel & Broekgaarden (2022) for a thorough review on both modeled and observed merger rates of compact objects). By looking deeper at the correlations between the source properties at a population level, we can begin to look for subpopulations of observations that we can confidently associate with a specific formation channel.

Isolated formation of compact binaries occurs in galactic fields, where two gravitationally bound stars isolated from their environment undergo standard main sequence evolution, each eventually forming into a compact object. Energy loss from GW radiation causes the binary to inspiral, which can eventually lead to merger; however, in order for the binary to merge within a Hubble time, the initial orbital separation of the compact objects must be small (Bavera et al. 2020; Mandel & Broekgaarden 2022). Some process during stellar evolution is therefore required to rapidly decrease the orbital separation down to this limit for systems with much larger ini-

jaxeng@uoregon.edu

tial separations. One proposed mechanism is the "common envelope phase", in which a cloud of non-rotating gas engulfs the two objects (typically after one star has already collapsed into a compact object) and drag forces quickly dissipate orbital energy, thus reducing the orbital separation enough so that the resulting compact binary can merge due to GW emission alone (Belczynski et al. 2016). In dynamical formation scenarios, scattering or exchange interactions between astrophysical bodies in a dense stellar environment are thought to produce binaries capable of merging within a Hubble time (Rodriguez et al. 2016a). There are many theorized models for the main physical processes that contribute to isolated and dynamical formation, but there are few robust and direct predictions of observable quantities from these models. Instead, current predictions of merger rates and population distributions are estimated from numerical simulations, which have large uncertainties due to uncertain underlying physics or poorly constrained initial conditions (Mandel & Broekgaarden 2022; Bavera et al. 2020; Giacobbo & Mapelli 2018; Dominik et al. 2013).
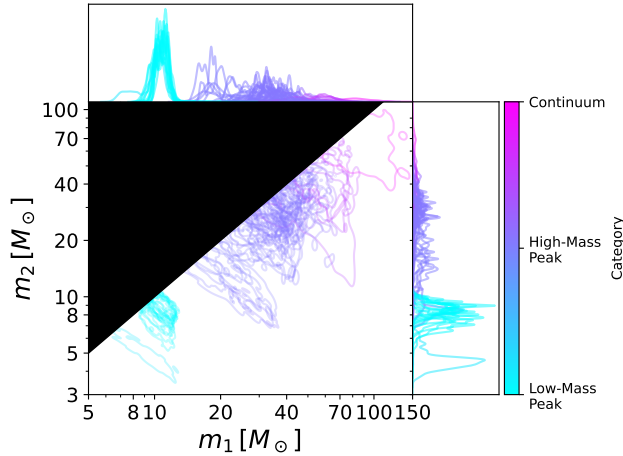

Figure 1.

The spin distribution of merging binaries is thought to provide the most direct evidence of their formation channel (Farr et al. 2017, 2018). Isolated binary evolution scenarios predict component spins to be near zero and preferentially aligned with the orbital angular momentum of the binary, though there are processes, such as angular momentum transport and supernova kicks, that can impart a small non-zero and modestly misaligned spin to one or both of the binary objects (Zevin & Bavera 2022; Belczynski et al. 2020; Bavera et al. 2020, 2021). On the other hand, systems assembled dynamically in stellar clusters are thought to have no
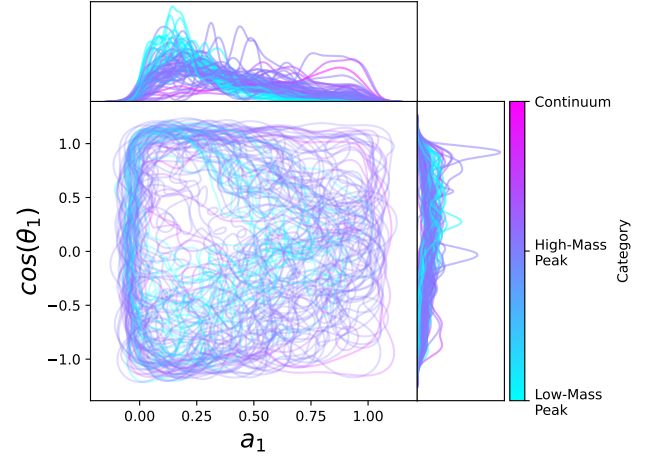

Figure 2.

preferential alignment, producing an isotropically distributed spin tilt distribution (Rodriguez et al. 2016b, 2019). With current data it is difficult to distinguish between these two channels, though studies have at least shown that GWTC-3 is not consistent with entirely dynamical or entirely isolated formation (The LIGO Scientific Collaboration et al. 2021b; Callister et al. 2022; Tong et al. 2022; Edelman et al. 2022b; Fishbach et al. 2022). Recent studies have found support for a significant contribution of systems formed through dynamical assembly in the population of BBHs inferred from the GWTC-2 and GWTC-3 catalogs (Abbott et al. 2021b; Roulet et al. 2021; The LIGO Scientific Collaboration et al. 2021b; Callister et al. 2022; Galaudage et al. 2021; Tong et al. 2022; Vitale et al. 2022a; Edelman et al. 2022b), though with large uncertainties.

While spin may be the characteristic most directly linked to compact binary formation history, the LVK parameter estimation of individual event spin properties contains large uncertainties, making it difficult to disentangle competing formation channels with spin alone. However, the component masses of individual events are typically inferred with greater certainty than their spin, and there are even features in the mass distribution that may signal the existence of different subpopulations (Tiwari & Fairhurst 2021; Edelman et al. 2022a; The LIGO Scientific Collaboration et al. 2021b; Tiwari 2022; Edelman et al. 2022b). Unfortunately, it can also be challenging to distinguish between the isolated and dynamical formation channels using only component mass, as the models in both scenarios predict masses that significantly overlap (Rodriguez et al. 2016c). Instead, a search for correlated population properties across mass, spin, and redshift may prove to be much more fruitful in distinguishing between the different CBC formation

channels (Fishbach et al. 2021; Callister et al. 2021; van Son et al. 2022; Biscoveanu et al. 2022).

In this letter, we search for signs of possible BBH subpopulations in GWTC-3 by incorporating discrete latent variables in the hierarchical Bayesian inference framework to probabilistically assign each BBH observation into separate categories that are associated with distinctly different mass and spin distributions. Incorporating these discrete variables during inference allows us to easily infer each BBH's association with each category, in addition to the posterior distributions for astrophysical branching ratios. The remaining sections of letter are structured as follows: Section 2 describes the statistical framework with the inclusion of discrete latent variables and the specific models used for separate subpopulations. Section 3 presents the results of our study, including the inferred branching ratios and the inferred subpopulation membership probabilities for each BBH in GWTC-3. In section 4 we discuss the implications of our findings and how it relates to the current understanding of compact binary formation and population synthesis. We finish in section 5, with a summary of the letter and prospects for distinguishing subpopulations in future catalogs after the LVK's fourth observing run.

2. METHODS

2.1. *Statistical Framework*

We employ the typical hierarchical Bayesian inference framework to infer the properties of the population of merging compact binaries given a catalog of observations. The rate of compact binary mergers is modeled as an inhomogeneous Poisson point process (Mandel et al. 2019), with the merger rate per comoving volume V_c (Hogg 1999), source-frame time T_{src} and binary parameters θ defined as:

$$\frac{dN}{dV_c dt_{\mathrm{src}} d\theta} = \frac{dN}{dV_c dt_{\mathrm{src}}} p(\theta|\Lambda) = \mathcal{R} p(\theta|\Lambda) \qquad (1)$$

with $p(\theta|\Lambda)$ the population model, $\mathcal{R}$ the merger rate, and Λ the set of population hyperparameters. Following other population studies (Mandel et al. 2019; Vitale et al. 2022b; Abbott et al. 2021c; The LIGO Scientific Collaboration et al. 2021c), we use the hierarchical likelihood that incorporates selection effects and marginalizes over the merger rate as:

$$\mathcal{L}(\boldsymbol{d}|\Lambda) \propto \frac{1}{\xi(\Lambda)} \prod_{i=1}^{N_{\mathrm{det}}} \int d\theta \mathcal{L}(d_i|\theta) p(\theta|\Lambda) \qquad (2)$$

Above, $\boldsymbol{d}$ is the set of data containing N_{det} observed events, $\mathcal{L}(d_i|\theta)$ is the individual event likelihood function for the ith event given parameters θ and $\xi(\Lambda)$ is the

fraction of merging binaries we expect to detect, given a population described by Λ. The integral of the individual event likelihoods marginalizes over the uncertainty in each event's binary parameter estimation, and is calculated with Monte Carlo integration and by importance sampling, reweighing each set of posterior samples to the likelihood. The detection fraction is calculated with:

$$\xi(\Lambda) = \int d\theta p_{\mathrm{det}}(\theta) p(\theta|\Lambda) \qquad (3)$$

with $p_{\mathrm{det}}(\theta)$ the probability of detecting a binary merger with parameters θ. We calculate this fraction using simulated compact merger signals that were evaluated with the same search algorithms that produced the catalog of observations. With the signals that were successfully detected, we again use Monte Carlo integration to get the overall detection efficiency, $\xi(\Lambda)$.

To model different subpopulations that could exist in the population, we use discrete latent variables that probabilistically associate each binary merger with different models. To model M subpopulations in a catalog of N_{det} detections, we add a latent variable q_i for each merger that can be M different discrete values, each associated with a separate model, $p_M(\theta|\Lambda)$, and hyperparameters, Λ_M. Evaluating the model (or hyper-prior) for the ith event with binary parameters, θ_i, given latent variable q_i and hyperparameters Λ_M, we have:

$$p(\theta_i|\Lambda, q_i) = p_{M=q_i}(\theta_i|\Lambda_{M=q_i}) \qquad (4)$$

To construct our probabilistic model, we first sample $p_M \sim \mathcal{D}(M)$, from an M-dimensional Dirichlet distribution of equal weights, representing the astrophysical branching ratios of each subpopulation. Then each of the N_{det} discrete latent variables are sampled from a categorical distribution with each category M having probability, p_M. Within the NUMPYRO (Bingham et al. 2018; Phan et al. 2019) probabilistic programming language, we use the implementation of the DiscreteHMCGibbs (Liu 1996) to sample the discrete latent variables, while using the NUTS (Hoffman & Gelman 2011) sampler for continuous variables. While this approach may seem computationally expensive, we find that the conditional distributions over discrete latent variables enable Gibbs sampling with similar costs and speeds to the equivalent approach that marginalizes over each discrete latent variable, q_i. We find the same results with either approach and only slight performance differences that depend on specific model specifications, and thus opt for the approach without marginalization. This method also has the advantage that we get posterior distributions on each event's subpopulation assignment without extra steps.

2.2. *Astrophysical Mixture Models*

For this study, we focus on one collection of primary mass and spin models to divide the BBH population into $M = 3$ potential subpopulations. Throughout this work, we refer to these three categories by their mass models as Low-Mass Peak, Mid-Mass Peak, and Continuum. For all three categories, the spin magnitude and tilt distributions of each component are assumed to be independently and identically distributed (IID), i.e. we use a single model and parameters for each binary spin per category. To reduce the number of free parameters and thus computational cost, we fix the power law slope of the merger rate with redshift to $\lambda_z = 2.7$ and use the same mass ratio model across all categories. We make use of the mass and spin basis spline (B-Spline) models from Edelman et al. (2022b). All the models and formalism used in our analysis are available in the GWInferno python library, along with the code and data to reproduce this study in this GitHub repository.

Given the recent evidence for a $10M_\odot$ and $35M_\odot$ peak in the BBH primary mass distribution (The LIGO Scientific Collaboration et al. 2021c; Tiwari 2022; Fishbach & Holz 2017; Talbot & Thrane 2018; Abbott et al. 2019c, 2021b), we chose to use a similar primary mass model to the Multi Peak and Multi Spin models in Abbott et al. (2021b), except we replace their power law mass component and parametric spin description with non-parametric B-Spline functions. We did this in order to avoid the model dependent biases on our resulting total distribution that we noticed were present when we used a power law.

We infer the mean $\mu_{m,M}$ and standard deviation $\sigma_{m,M}$ of each Gaussian peak. $M = 0$ denotes the peak with the lowest mean, Low-Mass Peak, and $M = 1$ denotes the one with the larger mean, Mid-Mass Peak. To keep the ordering of the peaks consistent during inference, we use a unique prior to draw the peak means $\mu_{m,0}, \mu_{m,1}$. In particular, we sample from a 3-dimensional Dirichlet distribution $\mathcal{D}(3)$ with equal weights, then cumulatively sum the sampled array. We discard the last value, since it is always 1, and the remaining two values are rescaled to primary mass m_1 and assigned to $\mu_{m,0}$ and $\mu_{m,1}$.

- Low-Mass Peak, $M = 0$ (JG: NUMBER parameters). This category assumes a truncated Gaussian model in primary mass, a B-spline model in spin magnitude a_i, and a B-spline model in

$cos(\theta_{\text{tilt}})$.

$$p_{m,0}(m_1|\Lambda_{m,0}) = G(m_1|\mu_{m,0}, \sigma_{m,0}) \quad (5)$$
$$p_{a,0}(a_i|\Lambda_{a,0}) = B_k(a_i|\mathbf{c}_{a,0}) \quad (6)$$
$$p_{\theta,0}(cos(\theta_i)|\Lambda_{\theta,0}) = B_k(cos(\theta_i)|\mathbf{c}_{\theta,0}) \quad (7)$$

- Mid-Mass Peak, $M = 1$ (JG: NUMBER parameters). Same form as Low-Mass Peak, except the mean $\mu_{m,1}$ of the primary mass truncated Gaussian model is required to be larger than $\mu_{m,0}$.

$$p_{m,1}(m_1|\Lambda_{m,1}) = G(m_1|\mu_{m,1}, \sigma_{m,1}) \quad (8)$$
$$p_{a,1}(a_i|\Lambda_{a,1}) = B_k(a_i|\mathbf{c}_{a,1}) \quad (9)$$
$$p_{\theta,1}(cos(\theta_i)|\Lambda_{\theta,1}) = B_k(cos(\theta_i)|\mathbf{c}_{\theta,1}) \quad (10)$$

- Continuum, $M = 2$ (JG: NUMBER parameters). The spin models are the same as the previous two categories, but now the primary mass is modeled with a B-spline function.

$$\log p_{m,2}(m_1|\Lambda_{m,2}) = B_k(m_1|\mathbf{c}_{m,2}) \quad (11)$$
$$p_{a,2}(a_i|\Lambda_{a,2}) = B_k(a_i|\mathbf{c}_{a,2}) \quad (12)$$
$$p_{\theta,2}(cos(\theta_i)|\Lambda_{\theta,2}) = B_k(cos(\theta_i)|\mathbf{c}_{\theta,2}) \quad (13)$$

3. RESULTS

- Start by introducing the dataset (GWTC-3) and threshold/cuts on catalog for our dataset

- Show results of main run model – mass dist – spin dists etc

- Discuss more specific details on different subpopulation mass/spin dists

- Talk about astrophysical branching ratios of subpopulations and which observations were "put" within each of the subpops

- Quantitative statements on spin mag dist of our isolated subpopulation

- Quantitative statements on spin orientation dist of our isolated subpop. How much does it prefer aligned spins over the other subpops?

With these models and framework in hand, we infer the mass and spin distributions with the recently released LVK catalog of gravitational wave observations, GWTC-3 JG: CITE THIS. We perform the same BBH threshold cuts on the catalog done by the LVK's accompnaying population analysis JG: CITE THIS, which leaves us with 70 BBH mergers. Additionally, we choose
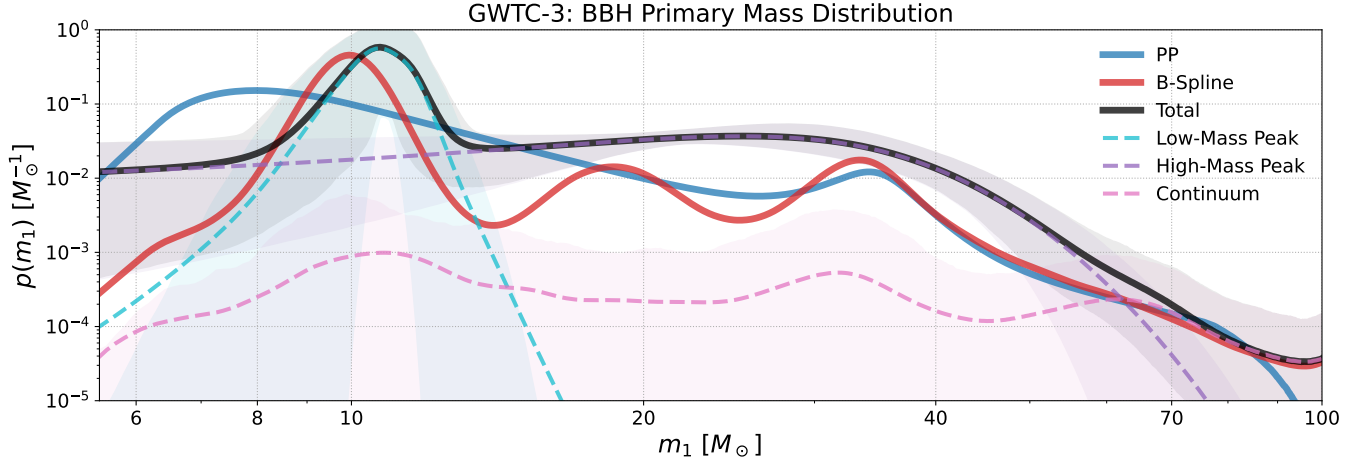
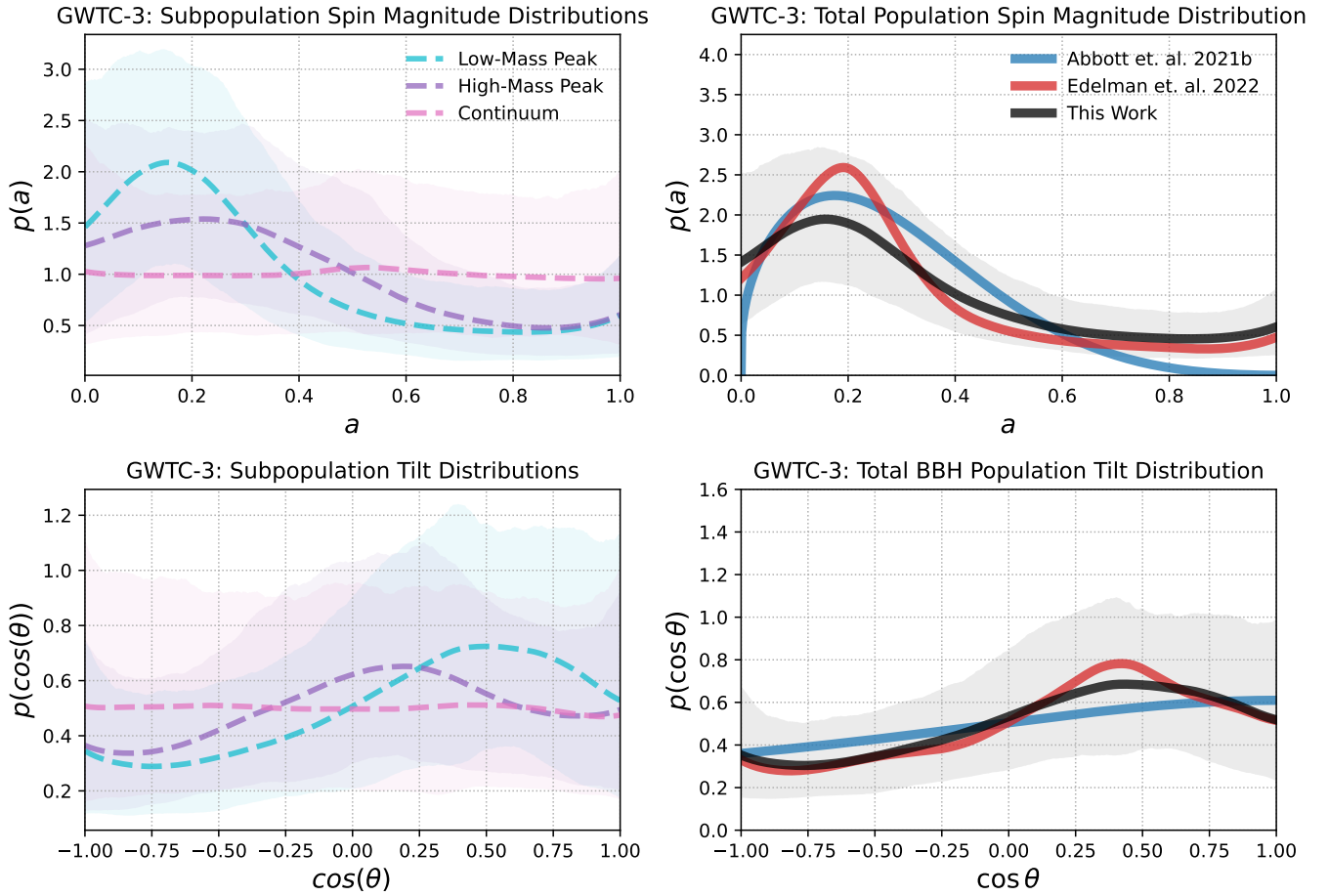**Figure 3.** The marginal primary mass distribution

Figure 4. The marginal primary spin magnitude distribution

to remove GW190814 from our anlaysis, as it is likely to be an outlier of the total BBH population and is not very well understood JG: CITE THIS. With the 69 remaining events, we are able to infer the mass and spin distribu-

tions of three potential BBH subpopulations, detailed below. $m_{\mathrm{LM,max}} = 11^{+0.83}_{-0.95}$

3.1. *BBH Mass and Spin Distributions*

Figure 3 shows the inferred total primary mass distribution, as well as the distributions of the three subpopulations, Low-Mass Peak, Mid-Mass Peak, and Continuum. For comparison, it also includes the primary mass distributions inferred by JG: CITE LVK GWTC-3 POP and JG: CITE BRUCE. Figure
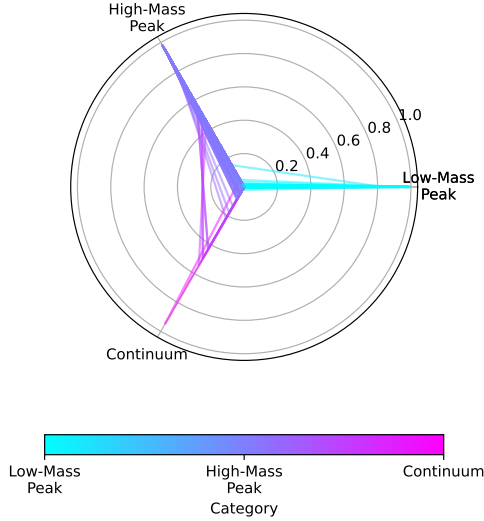
Figure 5.

4. ASTROPHYSICAL INTERPRETATION

- What can this new identified subpop help to enlighten in stellar pop synth community?

- can we use spin tilt dist to make statements on supernovae kicks in isolated formation?

- How does this compare to LVK work and other recent work? Are our results consistent or in conflict with dyn/iso fractions?

- report fdyn / fhm and etc

5. CONCLUSION

- Reiterate the motivation of the work

- restate the main conclusions leading us to identify this 10 solar mass peak as isolated

- briefly comment on main astro implications from prev section

- Discuss further work on other ways we can use this method to probe formation channels even deeper. (use spin vs mass dist to disentangle the sub pops. i.e. isotropic tilt for dynamical – aligned tilt for isolated)

- Discuss other applications of discrete latent variables (label for BNS/NSBH/BBH, label for 1G/2G/3G etc)

6. ACKNOWLEDGEMENTS

REFERENCES

Abbott, B. P., Abbott, R., Abbott, T. D., et al. 2016, PhRvL, 116, 061102, doi: 10.1103/PhysRevLett.116.061102

—. 2019a, Physical Review X, 9, 031040, doi: 10.1103/PhysRevX.9.031040

—. 2019b, ApJL, 882, L24, doi: 10.3847/2041-8213/ab3800

—. 2019c, ApJL, 882, L24, doi: 10.3847/2041-8213/ab3800

Abbott, R., Abbott, T. D., Abraham, S., et al. 2021a, Physical Review X, 11, 021053, doi: 10.1103/PhysRevX.11.021053

—. 2021b, ApJL, 913, L7, doi: 10.3847/2041-8213/abe949

—. 2021c, ApJL, 913, L7, doi: 10.3847/2041-8213/abe949

Acernese, F., Agathos, M., Agatsuma, K., et al. 2015, Classical and Quantum Gravity, 32, 024001, doi: 10.1088/0264-9381/32/2/024001

Akutsu, T., Ando, M., Arai, K., et al. 2021, Progress of Theoretical and Experimental Physics, 2021, 05A102, doi: 10.1093/ptep/ptab018

Arca Sedda, M., Mapelli, M., Spera, M., Benacquista, M., & Giacobbo, N. 2020, ApJ, 894, 133, doi: 10.3847/1538-4357/ab88b2

Astropy Collaboration, Robitaille, T. P., Tollerud, E. J., et al. 2013, A&A, 558, A33, doi: 10.1051/0004-6361/201322068

Astropy Collaboration, Price-Whelan, A. M., Sipőcz, B. M., et al. 2018, AJ, 156, 123, doi: 10.3847/1538-3881/aabc4f

Astropy Collaboration, Price-Whelan, A. M., Lim, P. L., et al. 2022, ApJ, 935, 167, doi: 10.3847/1538-4357/ac7c74

Bavera, S. S., Fragos, T., Qin, Y., et al. 2020, A&A, 635, A97, doi: 10.1051/0004-6361/201936204

Bavera, S. S., Fragos, T., Zevin, M., et al. 2021, A&A, 647, A153, doi: 10.1051/0004-6361/202039804

Belczynski, K., Holz, D. E., Bulik, T., & O'Shaughnessy, R. 2016, Nature, 534, 512, doi: 10.1038/nature18322

Belczynski, K., Klencki, J., Fields, C. E., et al. 2020, A&A, 636, A104, doi: 10.1051/0004-6361/201936528

Bingham, E., Chen, J. P., Jankowiak, M., et al. 2018, arXiv e-prints, arXiv:1810.09538. https://arxiv.org/abs/1810.09538

Biscoveanu, S., Callister, T. A., Haster, C.-J., et al. 2022, ApJL, 932, L19, doi: 10.3847/2041-8213/ac71a8

Bradbury, J., Frostig, R., Hawkins, P., et al. 2018, JAX: composable transformations of Python+NumPy programs, 0.3.13. http://github.com/google/jax

Callister, T. A., Haster, C.-J., Ng, K. K. Y., Vitale, S., & Farr, W. M. 2021, ApJL, 922, L5, doi: 10.3847/2041-8213/ac2ccc

Callister, T. A., Miller, S. J., Chatziioannou, K., & Farr, W. M. 2022, ApJL, 937, L13, doi: 10.3847/2041-8213/ac847e

Dominik, M., Belczynski, K., Fryer, C., et al. 2013, ApJ, 779, 72, doi: 10.1088/0004-637X/779/1/72

Edelman, B., Doctor, Z., Godfrey, J., & Farr, B. 2022a, ApJ, 924, 101, doi: 10.3847/1538-4357/ac3667

Edelman, B., Farr, B., & Doctor, Z. 2022b, arXiv e-prints, arXiv:2210.12834. https://arxiv.org/abs/2210.12834

Farr, B., Holz, D. E., & Farr, W. M. 2018, ApJL, 854, L9, doi: 10.3847/2041-8213/aaaa64

Farr, W. M., Stevenson, S., Miller, M. C., et al. 2017, Nature, 548, 426, doi: 10.1038/nature23453

Fishbach, M., & Holz, D. E. 2017, ApJL, 851, L25, doi: 10.3847/2041-8213/aa9bf6

Fishbach, M., Kimball, C., & Kalogera, V. 2022, ApJL, 935, L26, doi: 10.3847/2041-8213/ac86c4

Fishbach, M., Doctor, Z., Callister, T., et al. 2021, ApJ, 912, 98, doi: 10.3847/1538-4357/abee11

Galaudage, S., Talbot, C., Nagar, T., et al. 2021, ApJL, 921, L15, doi: 10.3847/2041-8213/ac2f3c

Giacobbo, N., & Mapelli, M. 2018, MNRAS, 480, 2011, doi: 10.1093/mnras/sty1999

Harris, C. R., Millman, K. J., van der Walt, S. J., et al. 2020, Nature, 585, 357, doi: 10.1038/s41586-020-2649-2

Hoffman, M. D., & Gelman, A. 2011, arXiv e-prints, arXiv:1111.4246. https://arxiv.org/abs/1111.4246

Hogg, D. W. 1999, arXiv e-prints, astro. https://arxiv.org/abs/astro-ph/9905116

Hunter, J. D. 2007, Computing in Science and Engineering, 9, 90, doi: 10.1109/MCSE.2007.55

LIGO Scientific Collaboration, Aasi, J., Abbott, B. P., et al. 2015, Classical and Quantum Gravity, 32, 074001, doi: 10.1088/0264-9381/32/7/074001

Liu, J. S. 1996, Biometrika, 83, 681

Luger, R., Bedell, M., Foreman-Mackey, D., et al. 2021, arXiv e-prints, arXiv:2110.06271. https://arxiv.org/abs/2110.06271

Mandel, I., & Broekgaarden, F. S. 2022, Living Reviews in Relativity, 25, 1, doi: 10.1007/s41114-021-00034-3

Mandel, I., Farr, W. M., & Gair, J. R. 2019, MNRAS, 486, 1086, doi: 10.1093/mnras/stz896

Phan, D., Pradhan, N., & Jankowiak, M. 2019, arXiv e-prints, arXiv:1912.11554. https://arxiv.org/abs/1912.11554

Rodriguez, C. L., Chatterjee, S., & Rasio, F. A. 2016a, PhRvD, 93, 084029, doi: 10.1103/PhysRevD.93.084029

Rodriguez, C. L., Zevin, M., Amaro-Seoane, P., et al. 2019, PhRvD, 100, 043027, doi: 10.1103/PhysRevD.100.043027

Rodriguez, C. L., Zevin, M., Pankow, C., Kalogera, V., & Rasio, F. A. 2016b, ApJL, 832, L2, doi: 10.3847/2041-8205/832/1/L2

—. 2016c, ApJL, 832, L2, doi: 10.3847/2041-8205/832/1/L2

Roulet, J., Chia, H. S., Olsen, S., et al. 2021, PhRvD, 104, 083010, doi: 10.1103/PhysRevD.104.083010

Talbot, C., & Thrane, E. 2018, ApJ, 856, 173, doi: 10.3847/1538-4357/aab34c

The LIGO Scientific Collaboration, the Virgo Collaboration, the KAGRA Collaboration, et al. 2021a, arXiv e-prints, arXiv:2111.03606. https://arxiv.org/abs/2111.03606

—. 2021b, arXiv e-prints, arXiv:2111.03634. https://arxiv.org/abs/2111.03634

—. 2021c, arXiv e-prints, arXiv:2111.03634. https://arxiv.org/abs/2111.03634

Tiwari, V. 2022, ApJ, 928, 155,
doi: 10.3847/1538-4357/ac589a

Tiwari, V., & Fairhurst, S. 2021, ApJL, 913, L19,
doi: 10.3847/2041-8213/abfbe7

Tong, H., Galaudage, S., & Thrane, E. 2022, arXiv e-prints,
arXiv:2209.02206. https://arxiv.org/abs/2209.02206

van Son, L. A. C., de Mink, S. E., Callister, T., et al. 2022,
ApJ, 931, 17, doi: 10.3847/1538-4357/ac64a3

Virtanen, P., Gommers, R., Oliphant, T. E., et al. 2020,
Nature Methods, 17, 261, doi: 10.1038/s41592-019-0686-2

Vitale, S., Biscoveanu, S., & Talbot, C. 2022a, arXiv
e-prints, arXiv:2209.06978.
https://arxiv.org/abs/2209.06978

Vitale, S., Gerosa, D., Farr, W. M., & Taylor, S. R. 2022b,
in Handbook of Gravitational Wave Astronomy. Edited
by C. Bambi, 45, doi: 10.1007/978-981-15-4702-7_45-1

Zevin, M., & Bavera, S. S. 2022, ApJ, 933, 86,
doi: 10.3847/1538-4357/ac6f5d

Zevin, M., Pankow, C., Rodriguez, C. L., et al. 2017, ApJ,
846, 82, doi: 10.3847/1538-4357/aa8408